

APIO16 and AFIO16 Single-Event Effects (SEE) Report

Josh Cortman

This report covers the Heavy Ion Single Event Effects (SEE) testing of the radiation-hardened level translating I^2C , SMBUS, SPI I/O expander available as a 30krad variant (APIO16) and 300krad variant (AFIO16). SEE testing included Single Event Latch-up (SEL), Single Event Upset (SEU), and Single Event Transient (SET) testing up to an effective LET of $76.8 \text{ MeV}\cdot\text{cm}^2/\text{mg}$.

This testing was conducted on silicon revision A00 which is not the final production silicon revision due to a minor bug identified during initial characterization. A separate errata is available detailing the nature of this bug. SEE testing will be completed on the next silicon revision prior to final release of the APIO16 and AFIO16.



Contents

List of Figures	3
List of Tables	3
1 Device Description	4
2 Facilities Description	5
2.1 SEE Facility	5
3 Device Preparation	7
4 Test Instrumentation and Hardware	7
5 Radiation Test Conditions	10
6 Single Event Latch-up (SEL) Testing	10
6.1 SEL Test Setup and Procedure	10
6.2 SEL Results	10
7 Single Event Transient (SET) and Single Event Upset (SEU) Testing	11
7.1 SET/SEU Test Setup and Procedure	11
7.2 SET/SEU Results	11
8 Event Rate Calculations	14
9 Summary	16
10 Revision History	17
11 Legal	17
References	17



List of Figures

1	AxIO16 device pinout	4
2	LBNL Available Beams and Characteristics [1]	5
3	Map of LBNL 88-Inch Facility [2]	6
4	Example Coupon Board	7
5	Front-side of SEE test board	7
6	Back-side of SEE test board	7
7	SEE test board schematic	8
8	Coupon board schematic	9
9	Instrumentation	9
10	SEL setup (Front)	10
11	SEL setup (Rear)	10
12	Example SET Event	14
13	Example SET Event (Enhanced View)	14

List of Tables

1	Beam Configurations	10
2	SEL Runs	11
3	SET/SEU Runs	13
4	Measured Cross Sections	15
5	LEO Event Rate Calculations	15
6	GEO Event Rate Calculations	15

1 Device Description

The APIO16 and AFIO16 are radiation-hardened by design level translating I^2C , SMBUS, SPI I/O expanders which are ideally suited for space, medical imaging and other applications demanding radiation tolerance and high reliability. They are fabricated in a BiCMOS process utilizing proprietary radiation-hardening techniques, delivering high resiliency to Single-Event Effects (SEE) and Total Ionizing Dose (TID). The APIO16 and AFIO16 operating voltage and temperature range are 1.4 V to 5.5 V and -55 °C to +125 °C. They are capable of I^2C operation up to 1MHz (Fast mode plus) and SPI operation up to 25 MHz. The device pinout is shown in Figure 1.

The APIO16 and AFIO16 feature extensive circuit techniques throughout, including triple modular redundancy, self correcting digital circuits and Dual Interlocked storage Cell (DICE) latches to ensure a high level of immunity to single-event transients (SET) and single event upsets (SEU) without requiring additional redundant devices.

Throughout the remainder of this report, “AxIO16” will be used to refer to both the APIO16 and AFIO16.

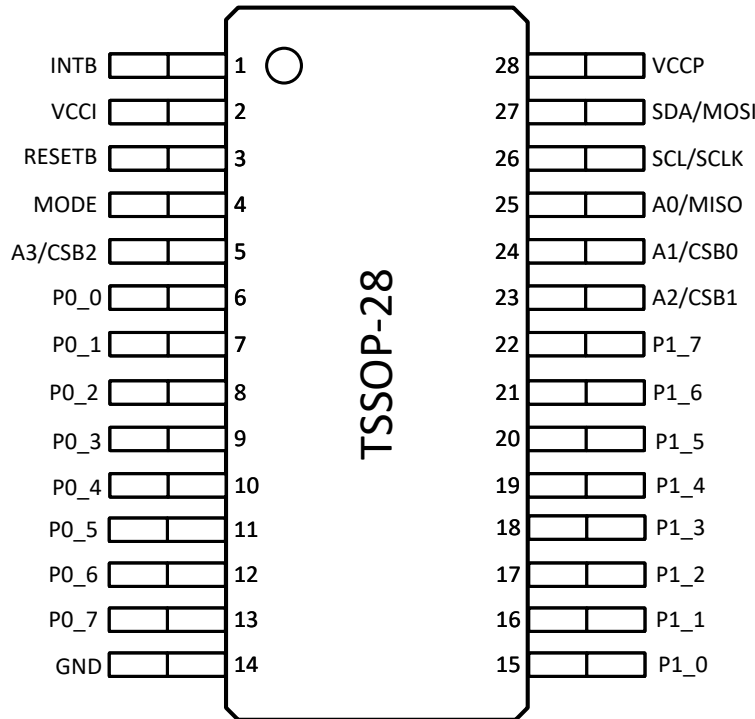


Figure 1: AxIO16 device pinout



2 Facilities Description

2.1 SEE Facility

The single event testing conducted in this report occurred November 11th through 15th, 2024 at Lawrence Berkeley National Laboratories (LBNL) using the 88-inch cyclotron. This facility is managed by the University of California for the United States Department of Energy. Berkeley Accelerator Space Effects (BASE) Facility is home to the 88-Inch Cyclotron. The 88-Inch Cyclotron is a 300-ton, K=140 sector-focused cyclotron with both light and heavy-ion capabilities. Protons and other light-ions are available at high intensities (10-20 pA) up to maximum energies of 60 MeV (protons), 65 MeV (deuterons), 170 MeV (3He), and 130 MeV (4He). Figure 2 shows a list of available ions.

Ion	Cocktail (AMeV)	Energy (MeV)	Z	A	Chg. State	% Nat. Abund.	LET 0° (MeV/mg/cm2)	LET 60° (MeV/mg/cm2)	Range (Max) (µm)
B	4.5	44.90	5	10	+2	19.9	1.65	3.30	78.5
N	4.5	67.44	7	15	+3	0.37	3.08	6.16	67.8
Ne	4.5	89.95	10	20	+4	90.48	5.77	11.54	53.1
Si	4.5	139.61	14	29	+6	4.67	9.28	18.56	52.4
Ar	4.5	180.00	18	40	+8	99.6	14.32	28.64	48.3
V	4.5	221.00	23	51	+10	99.75	21.68	43.36	42.5
Cu	4.5	301.79	29	63	+13	69.17	29.33	58.66	45.6
Kr	4.5	378.11	36	86	+17	17.3	39.25	78.50	42.4
Y	4.5	409.58	39	89	+18	100	45.58	91.16	45.8
Ag	4.5	499.50	47	109	+22	48.161	58.18	116.36	46.3
Xe	4.5	602.90	54	136	+27	8.9	68.84	137.68	48.3
Tb	4.5	724.17	65	159	+32	100	77.52	155.04	52.4
Ta	4.5	805.02	73	181	+36	99.988	87.15	174.30	53.0
Bi*	4.5	904.16	83	209	+41	100	99.74	199.48	52.9
B	10	108.01	5	11	+3	80.1	0.89	1.78	305.7
O	10	183.47	8	18	+5	0.2	2.19	4.38	226.4
Ne	10	216.28	10	22	+6	9.25	3.49	6.98	174.6
Si	10	291.77	14	29	+8	4.67	6.09	12.18	141.7
Ar	10	400.00	18	40	+11	99.6	9.74	19.48	130.1
V	10	508.27	23	51	+14	99.75	14.59	29.18	113.4
Cu	10	659.19	29	65	+18	30.83	21.17	42.34	108.0
Kr	10	885.59	36	86	+24	17.3	30.86	61.72	109.9
Y	10	928.49	39	89	+25	100	34.73	69.46	102.2
Ag	10	1039.42	47	107	+29	51.839	48.15	96.30	90.0
Xe	10	1232.55	54	124	+34	0.1	58.78	117.56	90.0
Au*	10	1955.87	79	197	+54	100	85.76	171.52	105.9
He*	16	43.46	2	3	+1	0.000137	0.11	0.22	1020.0
N	16	233.75	7	14	+5	99.63	1.16	2.32	505.9
O	16	277.33	8	17	+6	0.04	1.54	3.08	462.4
Ne	16	321.00	10	20	+7	90.48	2.39	4.78	347.9
Si	16	452.10	14	29	+10	4.67	4.56	9.12	274.3
Cl	16	539.51	17	35	+12	75.77	6.61	13.22	233.6
Ar	16	642.36	18	40	+14	99.600	7.27	14.54	255.6
V	16	832.84	23	51	+18	99.750	10.90	21.80	225.8
Cu	16	1007.34	29	63	+22	69.17	16.53	33.06	190.3
Kr	16	1225.54	36	78	+27	0.35	24.98	49.96	165.4
Xe*	16	1954.71	54	124	+43	0.1	49.29	98.58	147.9
C	20	240.00	6	12	+5	98.900	0.72	1.44	813.1
Ne	20	400.00	10	20	+8	90.480	2.00	3.99	504.5
Al	20	540.00	13	27	+11	100.000	3.36	6.72	428.7
Ar	20	800.00	18	40	+16	99.600	6.27	12.53	356.5
Cu	20	1260.00	29	65	+25	30.830	14.12	28.24	288.4
Kr	20	1560.00	36	78	+32	0.350	22.62	45.24	221.7
Y	20	1780.00	39	89	+36	100.000	24.82	49.64	229.2
Ag	20	2180.00	47	109	+44	48.161	34.24	68.48	212.9
Xe	20	2480.00	54	124	+47	0.100	45.40	90.80	193.8
N	30	425.45	7	15	+7	0.370	0.76	1.52	1370.0
O	30	490.22	8	17	+8	0.04	0.98	1.96	1220.0
Ne	30	620.00	10	21	+10	0.27	1.48	2.96	1040.0
Ar	30	1046.11	18	36	+17	0.337	4.87	9.74	578.1

*Special request only. **Ion isotopes and charge states subject to change without notice.
LETs calculated with SRIM using a silicon target in vacuum.

Figure 2: LBNL Available Beams and Characteristics [1]

SEE testing was conducted in Cave 4B in air. Figure 3 shows a map of the Lawrence Berkeley National Laboratory Cyclotron Facility, including Cave 4B. For dosimetry, five Hamamatsu R647 photomultiplier tubes (PMTs) are used. Four PMTs are placed around the edge of the beam, and one is placed in the middle. These PMTs are calibrated by Cyclotron operations staff. Just before a run, each ion is calibrated using the five PMTs. During the test, the center PMT is removed to permit exposure of the target. All PMTs currently use YAP:Ce crystals that have proven to show minimal, if any, degradation in performance after extended periods of time in high-flux, high-LET beams.

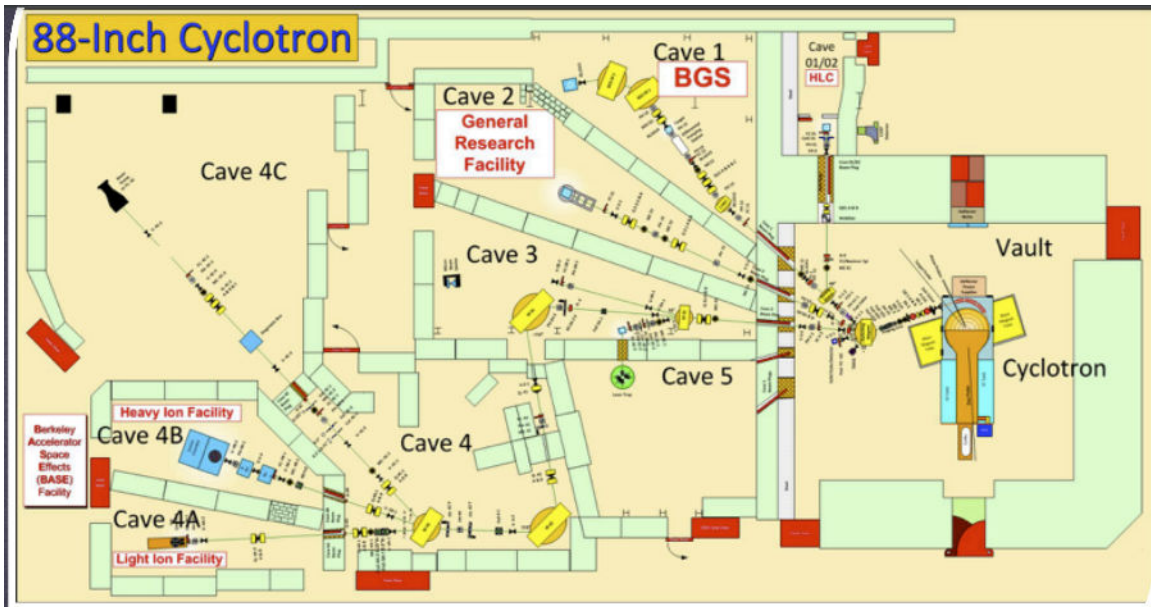


Figure 3: Map of LBNL 88-Inch Facility [2]

3 Device Preparation

The devices used for SEE testing were fabricated in GlobalFoundries' 180nm foundry. The devices were then packaged at QP technologies in Escondido, California. The devices were then mounted on coupon boards with probe access points and headers on the backside for connection to the SEE test board shown in Section 4. An example of one of the devices used for SEE testing is shown in Figure 4.

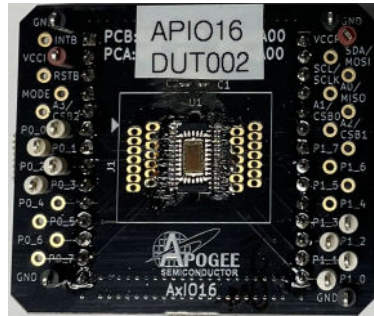


Figure 4: Example Coupon Board

4 Test Instrumentation and Hardware

For electrical biasing and test instrumentation interface, a custom SEE test board was designed by Apogee Semiconductor for the AxIO16. The front-side of the board, shown in Figure 5, has header pins for connection to the coupon boards. The front-side of the board was also covered with lead during testing to shield auxillary test components on the back-side (Figure 10). The back-side of the board, shown in Figure 6, contains relays, a Raspberry Pi, and additional auxiliary components used for communicating with the Device Under Test (DUT) via SPI and I2C during SEE testing.

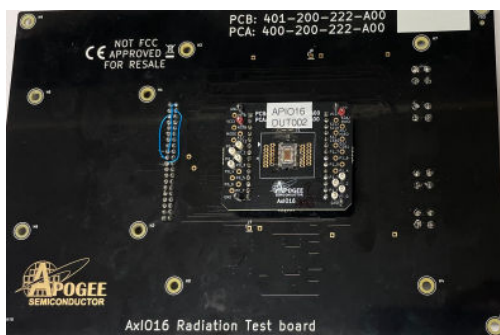


Figure 5: Front-side of SEE test board

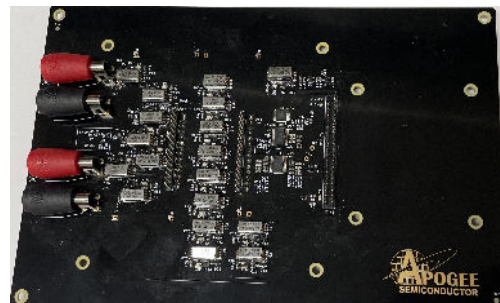


Figure 6: Back-side of SEE test board

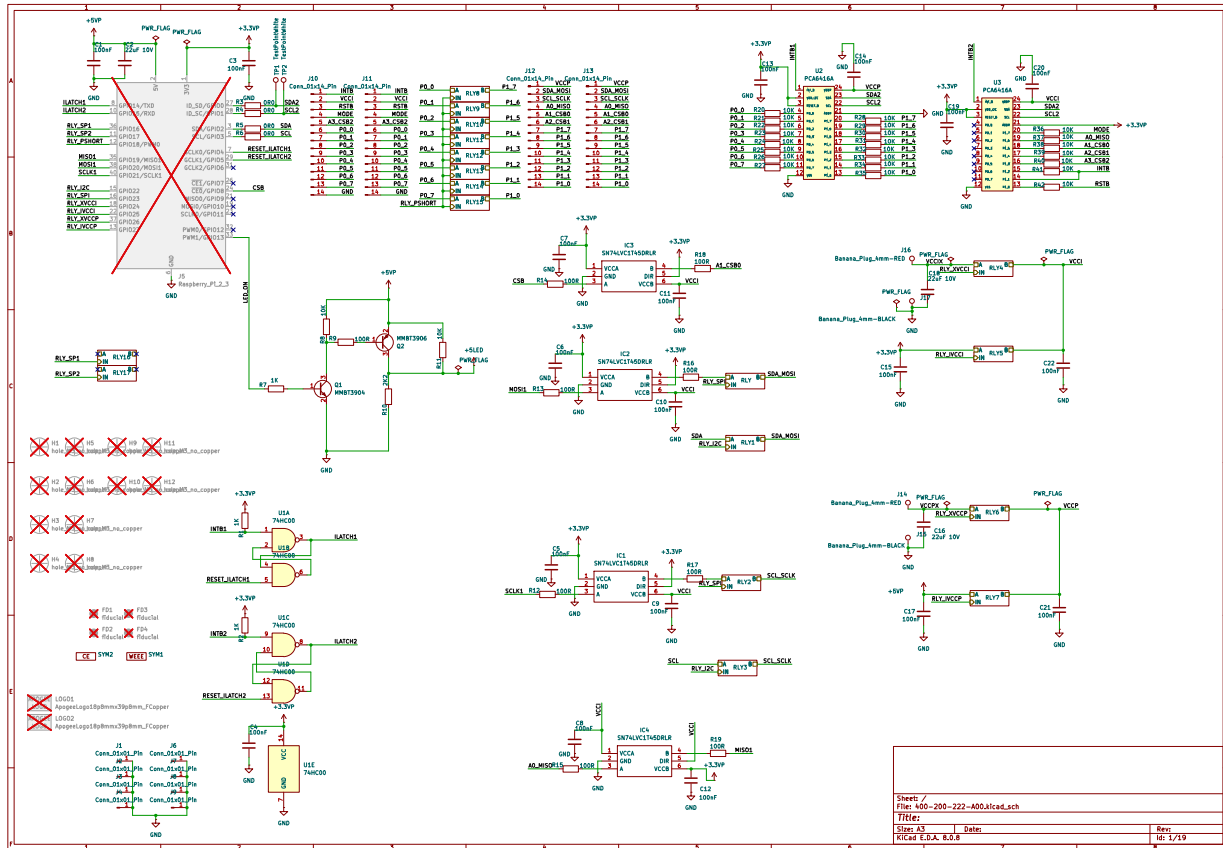
The schematic for the test board is shown in Figure 7. The DUT was configured in either a static or dynamic state during testing as defined below. Either SPI or I2C was used for communications. I2C communication was done at 1MHz. SPI communication frequency varied throughout testing, but was kept above 2MHz.

During static testing, the DUT was configured via SPI communication. Half of the I/Os on each port were configured as inputs and half were configured as outputs. Half the pins were then set high and half low by programming the DUT registers and providing external logic signals for the I/Os programmed as inputs. All registers of the DUT were then continually checked during testing and compared against their expected status.

During dynamic testing, the DUT was configured in a “loopback” configuration where one port was connected directly to the other. P0_0 was connected to P1_7, P0_1 was connected to P1_6, etc. At the start

of testing all port 0 pins were configured as outputs and all port 1 pins were configured as inputs. The port 0 output register was then set to 0x55. During testing, the port 0 output register was continually adjusted between 0x55 and 0xAA and immediately read back to verify it was programmed correctly. Each time the value was adjusted, the port 1 input port was read from the DUT and checked against the expected value. After every 1,000,000 writes, all registers were read and checked against the expected value, then the ports were flipped (port 1 programmed as an output and port 0 programmed as an input). If any communication errors or bit flips were detected, they were be logged.

The schematic for the coupon board is shown in Figure 8. The coupon board acts simply as a breakout board for the DUT with testpoints for monitoring the outputs during SET testing, decoupling capacitors for the supply pins, and headers for connecting to the SEE test board. Note that the Raspberry Pi shows as a “Do Not Populate” (DNP) component on the schematic, but was populated during testing.



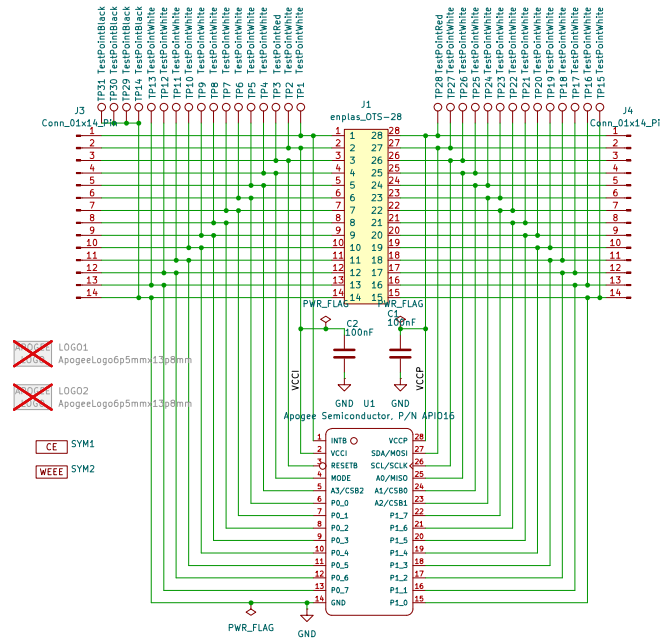


Figure 8: Coupon board schematic

The DUT and SEE test board components were powered by 2 external Keithley 2400 Source Measure Units (SMU). 2 Rohde & Schwarz MXO 4 series oscilloscopes were used for monitoring the DUT outputs during SET testing (1GHz and 200MHz). An additional XFR-100-12 power supply was also used to power the board components for some of the lower voltage SET testing. The test instrumentation is shown in Figure 9.

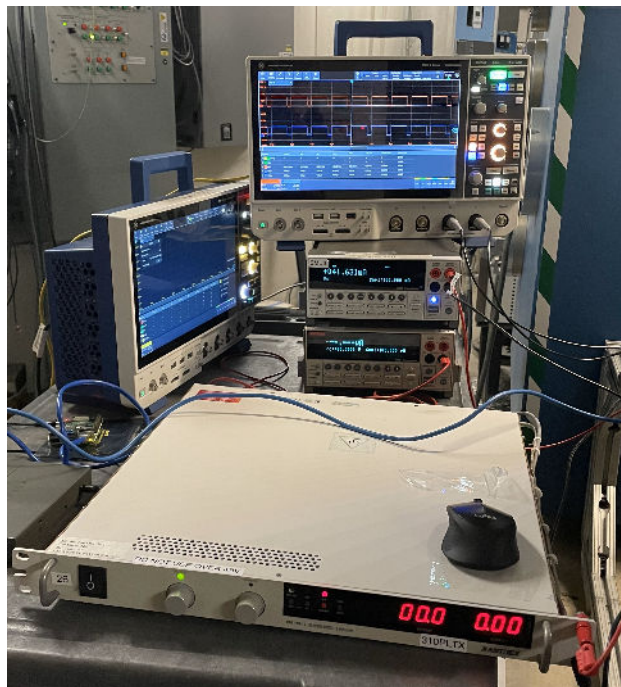


Figure 9: Instrumentation

5 Radiation Test Conditions

Exposure for SEE testing was completed in cave 4B at the LBNL facility. Xenon (Xe) and Krypton (Kr) were used with an air gap of 4 cm. The angle of incidence was varied to achieve different Effective Linear Energy Transfer (LET_{EFF}). SUESS 2024 software provided by Texas A&M Cyclotron Institute was used for calculations. Table 1 shows the various configurations used during testing.

Configuration	Ion	Air Gap (cm)	Angle of Incidence	Effective Range in Silicon (μm)	LET_{EFF} ($\text{MeV}\cdot\text{cm}^2/\text{mg}$)
1	^{124}Xe	4	40	68.7	76.8
2	^{124}Xe	4	26	80.6	65.5
3	^{124}Xe	4	0	89.7	58.9
4	^{78}Kr	4	45	74.6	42.7

Table 1: Beam Configurations

6 Single Event Latch-up (SEL) Testing

6.1 SEL Test Setup and Procedure

The DUT and test board were powered up to the maximum recommended power supply voltage (5.5 V) for both VCCI and VCCP using the two Keithley 2400 SMUs. The current was monitored at a sample rate of 3Hz. The device was then configured to a static state as defined in Section 4. A heat gun was used to increase the temperature of the DUT to the maximum recommended operating temperature (125°C). The temperature was then monitored remotely throughout testing with an IR camera to ensure the DUT remained within $\pm 3^\circ\text{C}$. The SEL test setup is shown in Figures 10 and 11.



Figure 10: SEL setup (Front)

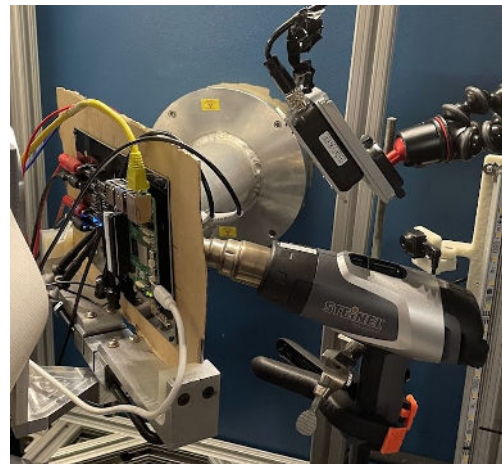


Figure 11: SEL setup (Rear)

6.2 SEL Results

SEL testing was conducted across 4 devices for an effective fluence of 1×10^7 ions $\cdot\text{cm}^2$ per DUT. No SEL events were observed across all runs. Table 2 shows a summary of all SEL runs.

Run Number	DUT	LET_{EFF} (MeV·cm ² /mg)	Average Effective Flux (ions·cm ² ·s)	Effective Fluence (ions·cm ²)	SEL events
23 & 24	2	76.8	1.37×10^4	1×10^7	0
25	5	76.8	1.36×10^4	1×10^7	0
26	7	76.8	2.84×10^4	1×10^7	0
27	8	76.8	2.92×10^4	1×10^7	0

Table 2: SEL Runs

7 Single Event Transient (SET) and Single Event Upset (SEU) Testing

7.1 SET/SEU Test Setup and Procedure

For SET and SEU testing the DUT was setup in either a static or dynamic configuration as defined in 4. When the DUT was in a static configuration, one oscilloscope was connected to an output driving logic high and the other oscilloscope was connected to an output driving logic low. An edge trigger was set to capture the waveform for any transients. SETs were defined as the output signal crossing the standard VIH and VIL levels for CMOS circuits: 30% VCCP for the logic low signals and 70% for the logic high signals. SEUs were defined as bit flips observed during testing where the actual value of a register did not match the expected value. During both static and dynamic testing, if the value read back from a register did not match the expected value, all register values were logged. All SET and SEU testing was completed at room temperature. Multiple voltage combinations for VCCI and VCCP were tested to determine the worst case. SPI mode was primarily used due to constraints of the test board. 2 dynamic runs (231 and 232) were completed using I2C mode.

7.2 SET/SEU Results

Table 3 shows a list of the SET/SEU test runs completed on the AxIO16. A total of 4 DUTs were used for SET/SEU testing. Each DUT was tested in both static and dynamic modes. No SEUs were observed across all runs on all devices. A total of 4 SET events were observed across all runs. These SET events occurred only with VCCI=1.4V and VCCP=5.5V on an output driving high. Every recorded transient had the same signature which consisted of a sudden spike dropping below the 70% VCCP threshold followed by a recovery back to the expected output level over about 1 μ s. The minimum recorded value for each transient was specified in parenthesis in the “SET Events” column. A full data set was not captured for the true transients which crossed the 70% VCCP threshold, but a similar event which stayed within the 70% VCCP threshold is shown in Figure 12 and 13.

The effective LET was reduced for runs 105-108 in attempt to find the onset of the transient. The transient was not seen during one full run at an effective LET of 42.7 MeV·cm²/mg, the onset for SETs was therefore determined to be 58.9 MeV·cm²/mg. The cross section did not increase with LET as expected, so a Weibull fit curve was not generated.

Run Number	DUT	LET_{EFF} (MeV·cm ² /mg)	Average Effective Flux (ions·cm ² ·s)	Effective Fluence (ions·cm ²)	Test Configuration (per Section 4)	VCCI (V)	VCCP (V)	SET Events	SEU Events
73	1	76.8	1.15×10^4	4.06×10^6	Static (SPI)	1.4	1.4	0	0
74	1	76.8	1.15×10^4	2.01×10^6	Static (SPI)	1.4	5.5	0	0

Preliminary



602-000-052-A00

Run Number	DUT	LET_{EFF} (MeV·cm ² /mg)	Average Effective Flux (ions·cm ² ·s)	Effective Fluence (ions·cm ²)	Test Configuration (per Section 4)	VCCI (V)	VCCP (V)	SET Events	SEU Events
75	1	76.8	1.15×10^4	2.01×10^6	Static (SPI)	1.4	5.5	0	0
76	1	76.8	1.15×10^4	2.01×10^6	Dynamic (SPI)	1.4	1.4	0	0
77	1	76.8	1.15×10^4	2.01×10^6	Dynamic (SPI)	1.4	5.5	0	0
78	1	76.8	1.15×10^4	2.01×10^6	Static (SPI)	5.5	5.5	0	0
79	1	76.8	1.15×10^4	2.01×10^6	Dynamic (SPI)	5.5	5.5	0	0
80	1	76.8	1.15×10^4	2.01×10^6	Static (SPI)	5.5	1.4	0	0
82	1	76.8	1.15×10^4	2.01×10^6	Dynamic (SPI)	5.5	1.4	0	0
83	1	76.8	1.15×10^4	2.01×10^6	Static (SPI)	1.4	5.5	1 (Min. 3.49V)	0
84	1	76.8	6.36×10^3	2.01×10^6	Static (SPI)	1.4	1.4	0	0
85	1	76.8	6.13×10^3	2.01×10^6	Dynamic (SPI)	3.3	3.3	0	0
86	1	76.8	6.13×10^3	2.01×10^6	Static (SPI)	3.3	3.3	0	0
93	10	76.8	1.15×10^4	2.01×10^6	Static (SPI)	1.4	1.4	0	0
94	10	76.8	1.15×10^4	2.01×10^6	Static (SPI)	1.4	5.5	1 (Min. 3.12V)	0
95	10	76.8	1.15×10^4	2.01×10^6	Dynamic (SPI)	1.4	5.5	0	0
96	10	76.8	1.15×10^4	2.01×10^6	Dynamic (SPI)	1.4	1.4	0	0
97	10	76.8	1.15×10^4	7.66×10^6	Static (SPI)	1.4	5.5	0	0
98	10	76.8	1.15×10^4	2.37×10^6	Static (SPI)	1.4	5.5	0	0
99	10	76.8	1.15×10^4	2×10^6	Static (SPI)	5.5	5.5	0	0
100	10	76.8	1.15×10^4	2×10^6	Dynamic (SPI)	5.5	5.5	0	0
101	10	76.8	1.15×10^4	2×10^6	Static (SPI)	5.5	1.4	0	0
102	10	76.8	1.15×10^4	2×10^6	Dynamic (SPI)	5.5	1.4	0	0
103	10	76.8	1.15×10^4	9.04×10^6	Static (SPI)	1.4	3.3	0	0
104	10	76.8	1.15×10^4	9.96×10^5	Static (SPI)	1.4	3.3	0	0
105	10	65.5	1.35×10^4	1.17×10^6	Static (SPI)	1.4	5.5	0	0
106	10	65.5	1.35×10^4	6.26×10^5	Static (SPI)	1.4	5.5	1 (Min. 3.32 V)	0
107	10	58.9	8×10^3	1×10^7	Static (SPI)	1.4	5.5	1 (Min. 3.2 V)	0
108	10	42.7	1.1×10^4	1×10^7	Static (SPI)	1.4	5.5	0	0
223	9	76.8	3.08×10^6	2.51×10^6	Static (SPI)	1.4	1.4	0	0



Run Number	DUT	LET_{EFF} (MeV·cm ² /mg)	Average Effective Flux (ions·cm ² ·s)	Effective Fluence (ions·cm ²)	Test Configuration (per Section 4)	VCCI (V)	VCCP (V)	SET Events	SEU Events
224	9	76.8	3.08×10^6	2.51×10^6	Static (SPI)	1.4	5.5	0	0
225	9	76.8	3.08×10^6	2.51×10^6	Dynamic (SPI)	1.4	5.5	0	0
226	9	76.8	3.08×10^6	2.51×10^6	Dynamic (SPI)	1.4	1.4	0	0
227	9	76.8	3.07×10^6	2.5×10^6	Static (SPI)	5.5	5.5	0	0
228	9	76.8	3.08×10^6	2.51×10^6	Dynamic (SPI)	5.5	5.5	0	0
229	9	76.8	3.08×10^6	2.51×10^6	Static (SPI)	5.5	1.4	0	0
230	9	76.8	3.08×10^6	2.51×10^6	Dynamic (SPI)	5.5	1.4	0	0
231	9	76.8	3.08×10^6	2.51×10^6	Dynamic (I2C)	3.3	3.3	0	0
232	4	76.8	3.07×10^6	2.5×10^6	Dynamic (I2C)	3.3	3.3	0	0
234	4	76.8	3.07×10^6	2.5×10^6	Static (SPI)	5.5	1.4	0	0
235	4	76.8	3.08×10^6	2.51×10^6	Dynamic (SPI)	5.5	1.4	0	0
236	4	76.8	3.07×10^6	2.5×10^6	Static (SPI)	5.5	5.5	0	0
237	4	76.8	3.08×10^6	2.51×10^6	Dynamic (SPI)	5.5	5.5	0	0
238	4	76.8	3.07×10^6	2.5×10^6	Static (SPI)	1.4	5.5	0	0
239	4	76.8	3.08×10^6	2.51×10^6	Dynamic (SPI)	1.4	5.5	0	0
240	4	76.8	3.08×10^6	2.51×10^6	Static (SPI)	1.4	1.4	0	0
241	4	76.8	3.07×10^6	2.5×10^6	Dynamic (SPI)	1.4	1.4	0	0

Table 3: SET/SEU Runs

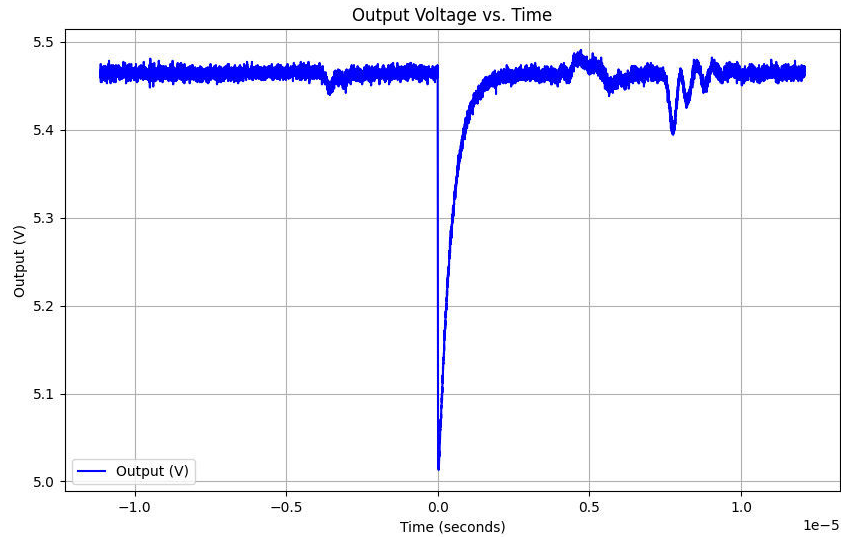


Figure 12: Example SET Event

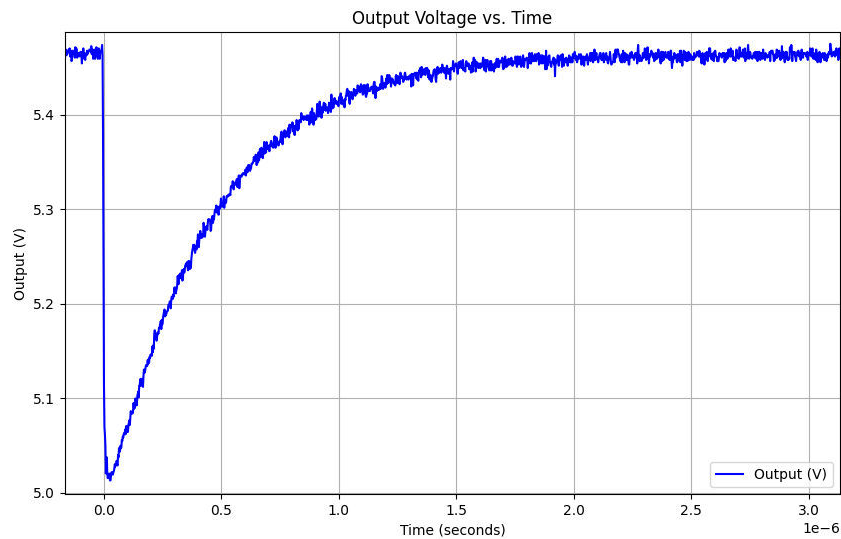


Figure 13: Example SET Event (Enhanced View)

8 Event Rate Calculations

Table 4 shows the calculated cross section for each type of SEE (SEU, SET, and SEL) based on the measured data. Tables 5 and 6 show cross sections and event rate calculations for LEO and GEO orbits respectively based on a 95% confidence interval. The “Estimated Flux at Event Onset” is the worst case integral flux for GEO and LEO orbits from the CREME96 model. The onset LET_{EFF} referenced for the integral flux value was 76.8 MeV·cm²/mg for SEU and SEL calculations and 58.9 MeV·cm²/mg for SET calculations since this was measured to be the onset for the SET events observed. The fluence used for SEL calculations was the total fluence of all SEL runs. The fluence used for SEU calculations was the total fluence for all runs completed at an LET_{EFF} of 76.8 MeV·cm²/mg since all of the device registers were checked during both



static and dynamic testing. The fluence used for SET calculations was the sum of all static runs completed at an LET_{EFF} of 76.8 MeV·cm²/mg. The total number of transients used for the SET calculations was the sum of transients seen at the maximum LET_{EFF} tested (2 events at 76.8 MeV·cm²/mg).

	SEU	SET	SEL
Total Fluence (ions·cm ²)	1.19×10^8	7.63×10^7	4×10^7
Total Transients	0	2	0
Actual Cross Section (cm ²)	0	2.62×10^{-8}	0

Table 4: Measured Cross Sections

	SEU	SET	SEL
Upper Bound Cross Section 95% confidence (cm ² /device)	3.09×10^{-8}	9.47×10^{-8}	9.22×10^{-8}
Estimated Flux at event onset	4.19×10^{-6}	1.39×10^{-5}	4.19×10^{-6}
Event rate (95% confidence) (Events/Day)	1.29×10^{-13}	1.32×10^{-12}	3.86×10^{-13}
Mean Time Between Events (95% confidence) (Years)	2.12×10^{10}	2.08×10^9	7.09×10^9

Table 5: LEO Event Rate Calculations

	SEU	SET	SEL
Upper Bound Cross Section 95% confidence (cm ² /device)	3.09×10^{-8}	9.47×10^{-8}	9.22×10^{-8}
Estimated Flux at event onset	1.56×10^{-4}	5.66×10^{-4}	1.56×10^{-4}
Event rate (95% confidence) (Events/Day)	4.82×10^{-12}	5.36×10^{-11}	1.44×10^{-11}
Mean Time Between Events (95% confidence) (Years)	5.69×10^8	5.11×10^7	1.9×10^8

Table 6: GEO Event Rate Calculations



9 Summary

The AxIO16 was characterized at Berkeley National Laboratory for Single Event Transient (SET), Single Event Upset (SEU), and Single Event Latch-up (SEL) performance using Krypton and Xenon with an Effective Linear Energy Transfer (LET_{EFF}) ranging from 42.7 MeV·cm²/mg to 76.8 MeV·cm²/mg. No SEU events were observed across 4 devices and a total fluence of 1.41×10^8 ions·cm². No SEL events were observed across 4 devices and a total fluence of 4×10^7 ions·cm². A total of 4 transients were observed across a total fluence of 1.41×10^8 ions·cm². The transients were observed only under one biasing condition ($V_{CCI}=1.4V$ and $V_{CCP}=5.5V$). The mean time between events was calculated for each type of SEE and the worst case mean time between events at a 95% confidence interval was determined to be 1.9×10^8 years for SEL in a GEO environment. These results demonstrate the robust SEE performance of the APIO16 and AFIO16 (Silicon revision A00) for both LEO and GEO environments.



10 Revision History

REVISION	DESCRIPTION	DATE
A00	Initial release.	February 7, 2025

11 Legal

All product, product specifications and data are subject to change without notice. Apogee Semiconductor provides technical data (such as datasheets), design resources (including reference designs), reliability data (including performance in radiation environments), application or other design advice, safety information, and other resources “as is” and with all faults, and disclaims all warranties, express and implied, including without limitation any implied warranties of merchantability, fitness for a particular purpose or non-infringement of third party intellectual property rights. These resources are intended for skilled engineers with understanding of high reliability and high radiation environments and its complexities. Apogee Semiconductor is not responsible for: (1) selecting the suitable products for a given application, (2) designing, verifying, validating and testing it, or (3) ensuring that it meets any performance, safety, security, or other requirements. These resources are subject to change without advance notice. The use of these resources is restricted to the development of an application that uses the Apogee Semiconductor products described in them. Other reproduction and display of these resources is prohibited. No license is granted to any other Apogee Semiconductor intellectual property right or to any third-party intellectual property right. Apogee Semiconductor disclaims responsibility and reserves the right to demand indemnification for any claims, damages, costs, losses, and liabilities arising out of wrongful use of these resources. The products are provided subject to Apogee Semiconductor’s [Terms of Sale \(https://www.apogeesemi.com/terms\)](https://www.apogeesemi.com/terms) or other applicable terms provided in conjunction with applicable products. The provision of these resources does not expand or otherwise alter applicable warranties or warranty disclaimers for Apogee Semiconductor products. Purchasers of these products acknowledge that they may be subject to and agree to abide by the United States laws and regulations controlling the export of technical data, computer software, electronic hardware and other commodities. The transfer of such items may require a license from the cognizant agency of the U.S. Government.

References

- [1] Lawrence Berkeley National Laboratory, “Cocktails and Ions” [Online Resource], available at <https://cyclotron.lbl.gov/base-rad-effects/heavy-ions/cocktails-and-ions> (accessed February 6, 2025).
- [2] Lawrence Berkeley National Laboratory, “Beamline Map” [Online Image], available at <https://cyclotron.lbl.gov/beamline-map> (accessed February 6, 2025).
- [3] “Single Event Effects Test Method And Guidelines”, ESCC Basic Specification No. 25100, Oct. 2014.
- [4] D. Kececioglu, ”Reliability and Life Testing Handbook”, Vol. 1, PTR Prentice Hall, New Jersey,1993, pp. 186-193.
- [5] Vanderbilt University CREME96 Website <https://creme.isde.vanderbilt.edu/>
- [6] A. J. Tylka, J. H. Adams, P. R. Boberg, et al., “CREME96: A Revision of the Cosmic Ray Effects on Micro-Electronics Code”, Trans. on Nucl. Sci, 44(6), Dec. 1997, pp. 2150 – 2160.
- [7] “Test Procedures for the Measurement of Single-Event Effects in Semiconductor Devices from Heavy Ion Irradiation”, EIA/JESD57A, Nov. 2017.
- [8] “Measurement and Reporting of Alpha Particle and Terrestrial Cosmic Ray-Induced Soft Errors in Semiconductor Devices”, EIA/JESD89B, Sep. 2021